Electronic Supplementary Material (ESI) for Dalton Transactions.

The role of the metal center on charge transport rate in MOF-525: cobalt and nickel porphyrin

Pedro Arturo Herrera-Herrera,[ab] Erika Rodríguez-Sevilla [b] and Ana Sofía Varela *[a]

[a]Instituto de Química, Universidad Nacional Autónoma de México, Ciudad Universitaria, Circuito exterior s/n, Del. Coyoacán 04510, Ciudad de México.

[b]Laboratorio de nanosensores biofotónicos, Centro de Investigaciones en Óptica, A. C., Loma del bosque 115, Col. Lomas del Campestre, León, Guanajuato 37150, México.

Content

1. Experimental methods

1.1 Materials

The following materials were used for the synthesis and electrochemical characterization of MOF-525: Zirconyl chloride octahydrate ($ZrOCl_2 \cdot 8H_2O$) (Sigma-Aldrich, 98%), meso-tetrakis(4-carboxyphenyl)porphine ($H_4TCPP\text{-}H_2$) (Sigma-Aldrich), *N, N*-dimethylformamide (DMF) (Sigma-Aldrich, 99.8%), Benzoic acid (Merck, Reag. Ph Eur), Methanol (Sigma-Aldrich, HPLC), 4-aminobenzoic acid (PABA) (Sigma-Aldrich, 99%), sodium nitrite (JT Baker, RA ACS), Hydrochloric acid (Sigma-Aldrich, 37%), Acetonitrile (MeCN) (JT Baker, HPLC), tetrabutylammonium hexafluorophosphate ($TBAPF_6$) (Sigma-Aldrich, for electrochemical analysis ≥ 99.0%), Ferrocene (Sigma-Aldrich, 98%), molecular sieves, 3 Å beads (Sigma-Aldrich). $CoCl_2 \cdot 6H_2O$ (Sigma-Aldrich, ACS reagent, 98 %) and $NiCl_2 \cdot 6H_2O$ (Sigma-Aldrich, ReagentPlus®). Carbon paper: AvCarb® MGL370, 0.37 mm thickness and 78% of porosity.

1.2 Synthesis of MOF-525 in their powder form

The MOF-525 synthesis was carried out using a modified version of the method reported by Hod *et al.*[1] Namely, 105 mg of $ZrOCl_2 \cdot 8H_2O$ (0.30 mmol) and 2.7 g (22 mmol) of benzoic acid were mixed in 8 mL of DMF (in a 20 mL scintillation vial) and ultrasonically dissolved. The clear solution was incubated in a mineral oil bath (80 °C, 2 hours). After cooling down to room temperature 47 mg (0.06 mmol) of $H_4TCPP\text{-}H_2$ were added to this solution and the mixture was sonicated for 20 min. The suspension was heated in a mineral oil bath (70 °C, 48 hours). After cooling down to room temperature, the resulting purple-red polycrystalline material was isolated by filtration and washed 3 times with DMF and subsequently, the solid residue was washed three times with methanol and kept in methanol for additional 48 hours, replacing the methanol after the first 24 hours. Finally, the solvent was removed, and the MOF was activated at 80°C under vacuum for 12 hours.

1.3 Postmetalation of MOF-525 in their powder form

The metalation was carried out using the postsynthetic modification approach proposed by Morris *et al.*[2] with slight modifications. For this method 0.62 mmol of the corresponding salt ($CoCl_2 \cdot 6H_2O$ or $NiCl_2 \cdot 6H_2O$) were dissolved in 10 mL of DMF (in a 20 mL scintillation vial), later 50 mg of MOF-525 were added into the solution, which was then heated to 100°C for 48 hours in an aluminum heating block. After cooling down the material was isolated by

filtration and washed 3 times with DMF and subsequently, the solid residue was washed three times with methanol and kept in methanol for additional 48 hours, replacing the methanol after the first 24 hours. The solvent was removed, and the MOF was activated at 80°C under vacuum for 12 hours. The metallated MOFs with cobalt and nickel are named MOF-525@Co and MOF-525@Ni, respectively.

1.4 MOF-525 SURMOFs formation

A. Diazotization reaction: This method consists in the in-situ formation of 4-carboxibenzendiazonium cation in an aqueous electrolyte and the subsequent electrografting to a carbon paper electrode as reported by Balakrishnan *et al*.[3] and Hou *et al*[4]. In this method 1.19 g of 4-aminobenzoic acid (10 mmol) were dissolved by mixing 3 mL of concentrated hydrochloric acid (12 M) and 14 mL of water. A precipitate was obtained after cooling to 0 °C. This precipitate disappeared after slow addition of a solution containing 0.752 g of sodium nitrite (11 mmol) in 4 mL of water, forming a clear yellow solution, indicating the formation of the 4-carboxibenzendiazonium chloride[5]. After 20 minutes, the subsequent surface derivatisation was carried out by electrochemical reduction of the diazonium cation.

B. Aryl radical formation: For this step of the surface modification, we used a carbon paper electrode (1 cm x 3 cm) with an exposed area of 2 cm^2 as a working electrode, a Pt mesh counter electrode and a homemade Ag/AgCl (3.0 M KCl) as reference electrode. As electrolyte we used the previously obtained solution containing the diazonium cation. The surface modification was achieved by cyclic voltammetry between -1.0 to 1.0 V vs. Ag/AgCl (3.0 M KCl) at 100 mV s^{-1} (3 cycles). Following electrografting the functionalized electrode was washed with deionized water and air dried.

C. MOF film formation: The MOF was grown onto the modified electrodes following a similar synthesis as for the powder formation. We used 105 mg of $ZrOCl_2 \cdot 8H_2O$ (0.30 mmol) and 2.7 g (22 mmol) of benzoic acid, which were mixed in 8 mL of DMF (in a 20 mL scintillation vial) and ultrasonically dissolved. The clear solution was incubated in a mineral oil bath (80 °C, 2 hours). After cooling down to room temperature 47 mg (0.06 mmol) of $H_4TCPP\text{-}H_2$ were added to this solution and the mixture was sonicated for 20 min. The vial content was divided in two separate 20 mL scintillation vials and one functionalized electrode was immersed into the interior of each vial (in an inclined position). The vials were heated in a mineral oil bath (70 °C, 48 hours). After cooling down to room temperature, the obtained MOF films were removed and washed with 30 mL of DMF, three times with methanol and kept in methanol for additional 48 hours, replacing the methanol after the first 24 hours. Finally, the solvent was removed, and the MOF films were activated at 80°C under vacuum for 12 hours.

D. Metallation of MOF films: 18.4 mg of $CoCl_2 \cdot 6H_2O$ ($7.7x10^{-5}$ mol) or 18.3 mg of $NiCl_2 \cdot 6H_2O$ ($7.7x10^{-5}$ mol) were dissolved in 10 mL of DMF (in a 20 mL scintillation

vial). The MOF-525 film was immersed in the previous solution and the vial was heated to 100°C for 48 hours in an aluminum heating block. After cooling down the metallated SURMOF was washed with 30 mL of DMF, soaked in DMF for 24 hours. Then the solvent was exchanged for methanol where it is kept for additional 48 hours, replacing the methanol after the first 24 hours. The solvent was removed, and the metallated MOF film was activated at 80°C under vacuum for 12 hours. The metallated MOF films with cobalt and nickel were named MOF-525@Co and MOF-525@Ni films, respectively.

1.5. Electrochemical experiments

A. **Cyclic voltammetry**: The experiments were conducted in a Biologic SP-300 potentiostat. The working electrode was the corresponding metallated MOF film (exposed area = 2 cm^2), a Pt mesh as counter electrode and an Ag/AgCl (3.0 M KCl) electrode as reference electrode. We used 0.3 M of tetrabutylammonium hexafluorophosphate (*n*-Bu_4NPF_6) in acetonitrile (HPLC and dried with 3 Å molecular sieves) as electrolyte. Before cyclic voltammetry experiments, the electrolyte was saturated with high purity N_2 (previously saturated with acetonitrile vapours in pre-bubbler) for 10 minutes and the OCP monitored for 20 minutes (with N_2 in headspace). The cyclic voltammetry began from this potential and was stepped between -1.5 V and 0.350 V vs. Ag/AgCl (3.0 M KCl) at a scan rate between 1 and a 1000 mV s^{-1}. All experiments were conducted in N_2 atmosphere.

B. **Potential step chronoamperometry**: The sequence used for chronoamperometry consisted of maintaining a potential of 0.350 V vs. Ag/AgCl (3.0 M KCl) for 0.1 s and stepped to -1.5 V vs. Ag/AgCl (3.0 M KCl). At this potential 10 s of the chronoamperometric response were recorded. Then the potential was stepped back to 0.350 V vs. Ag/AgCl (3.0 M KCl) and 10 s of the chronoamperometric response were recorded. Before each measurement, the electrolyte was saturated with high purity N_2 (previously saturated with acetonitrile vapours in pre-bubbler) for 10 minutes and the OCP monitored for 20 minutes (with N_2 in headspace).

C. **Imidazole experiments:** For the imidazole experiments with MOF films, the corresponding (and activated) MOF-525@Co or MOF-525@Ni film was immersed in 10 mL of a 30 mM imidazole solution in acetonitrile. The solution was kept under stirring for 10 minutes with the aim of favouring chloride displacement from the porphyrin metal centers. Then the MOF film was transferred to the electrochemical cell which contained 30 mM of imidazole and 0.3 M *n*-Bu_4NPF_6 electrolyte. The cyclic voltammetry and potential step chronoamperometry were conducted as previously described.

1.6. Instrumentation

ATR-IR spectra were obtained in a Bruker Alpha ATR model. XRD diffraction patterns were obtained with a Bruker D8 Advance with Bragg-Brentano geometry, Cu Kα radiation, and Linxeye detector. The GIXD patterns were obtained in a Siemens D500 with grazing incidence attachment. UV-vis spectra were measured by an Agilent 8453 (for the measurement 1 mg of the MOF were digested with 1 mL of a 1.0 M KOH solution, from this suspension 100 µL were taken and diluted with 4 mL of deionized water). EDS and SEM micrographs were obtained by a field emission of high resolution, JEOL-JSM-7800F, the data was analysed using ImageJ software.

2. Supporting results

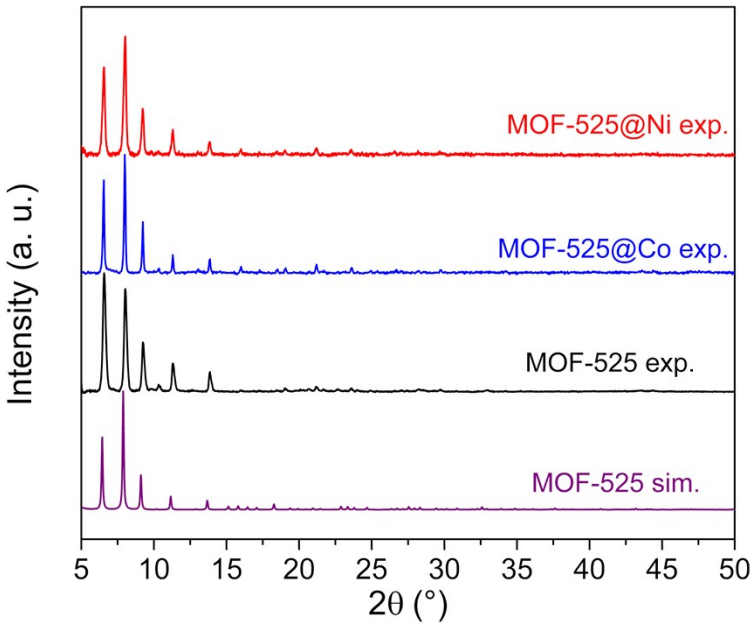

Fig. S1. PXRD patterns of simulated MOF-525, MOF-525, MOF-525@Co and MOF-525@Ni in their powder form confirming that the metalation process does not affect the crystal structure of MOF-525.

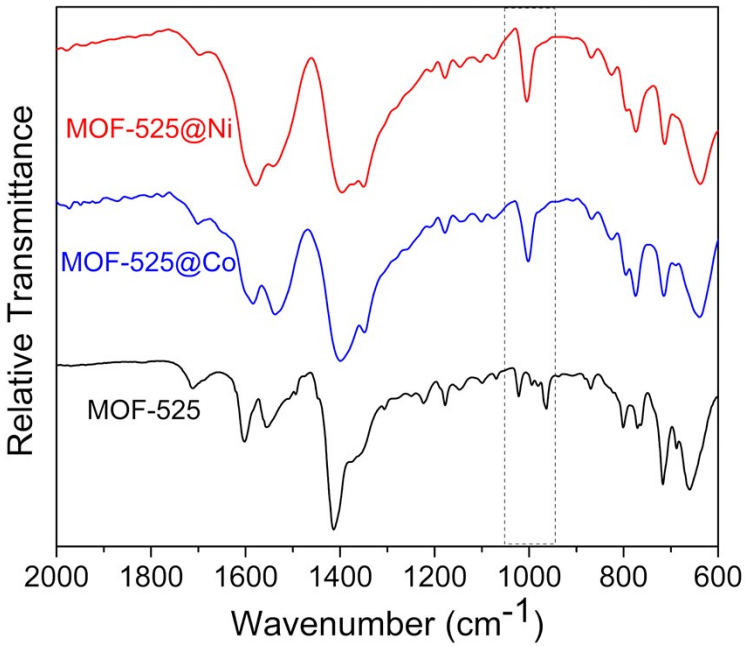

Fig. S2. ATR-IR spectra of MOF-525, MOF-525@Co and MOF-525@Ni in their powder form. The characteristic vibrations close to 1000 cm^{-1} are attributed to the rocking vibration of the C-H bonds of the pyrrole rings.[6] This vibration for MOF-525@Co and MOF-525@Ni displays one band as result of the planarity induced to the macrocycle from the incorporation of the metal center. This band is also associated with the Metal-nitrogen bond.[7]

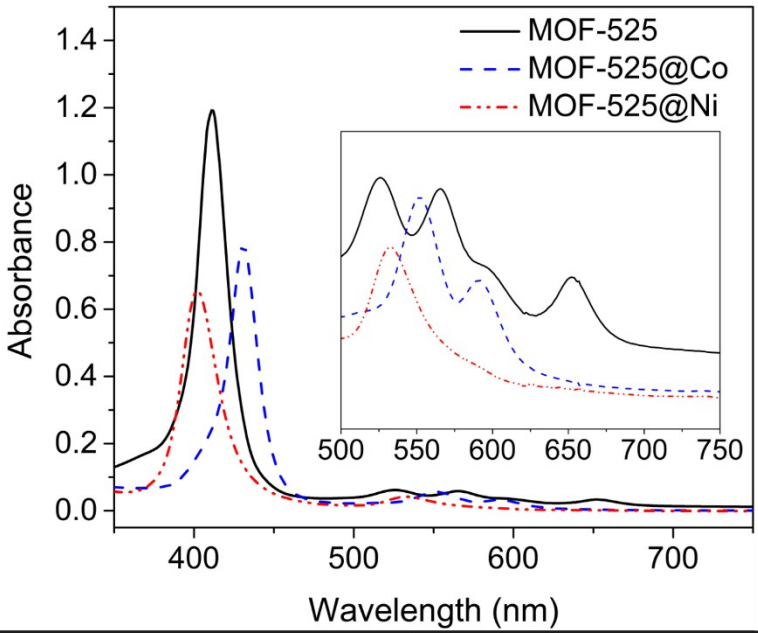

	Soret Band	Q bands			
MOF-525	411	526	565	598	652
MOF-525@Co	431	552	591		
MOF-525@Ni	402	532			

Fig. S3. UV-vis spectra of digested MOF-525, MOF-525@Co and MOF-525@Ni in their powder form. The decrease in the number of Q-bands in metalated MOF-525 with respect to unmetalated MOF-525 is the result of an increase in the local symmetry on the metalloporphyrin.[8]

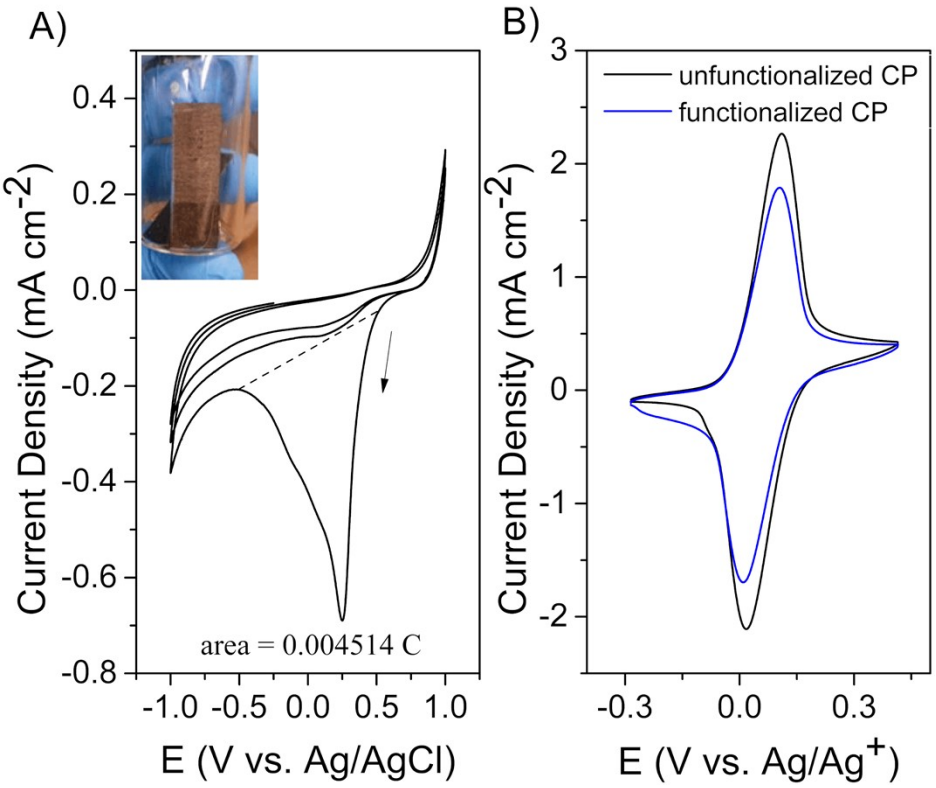

Fig. S4. A) Cyclic voltammogram of 4-carboxibenzendiazonium chloride showing the reduction peak for aryl radical formation, v = 100 mV s^{-1}, 3 cycles. The picture shows the surface of the carbon paper electrode after experiment. B) Cyclic voltammogram of ferrocene/ferrocenium as redox probe to corroborate the surface functionalization of the electrode, c = 1 mM ferrocene in 0.1 M n-Bu_4NPF_6, v = 100 mV s^{-1}. The effective functionalization of the surface was corroborated by comparing the cyclic voltammograms of the unfunctionalized and functionalized electrodes in ferrocene showing a depleted redox signal in the latter. This blocking behaviour can be explained by electrostatic interactions between the modified surface and the redox probe and electrolyte/solvent effects.[5]

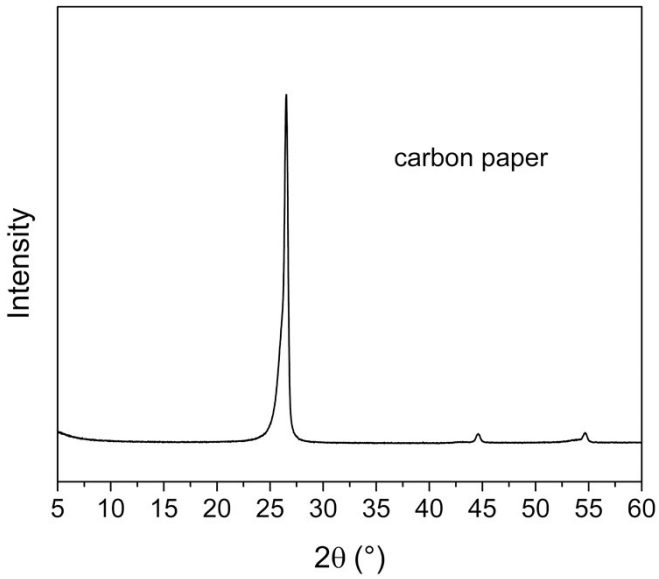

Fig. S5 XRD pattern of carbon paper.

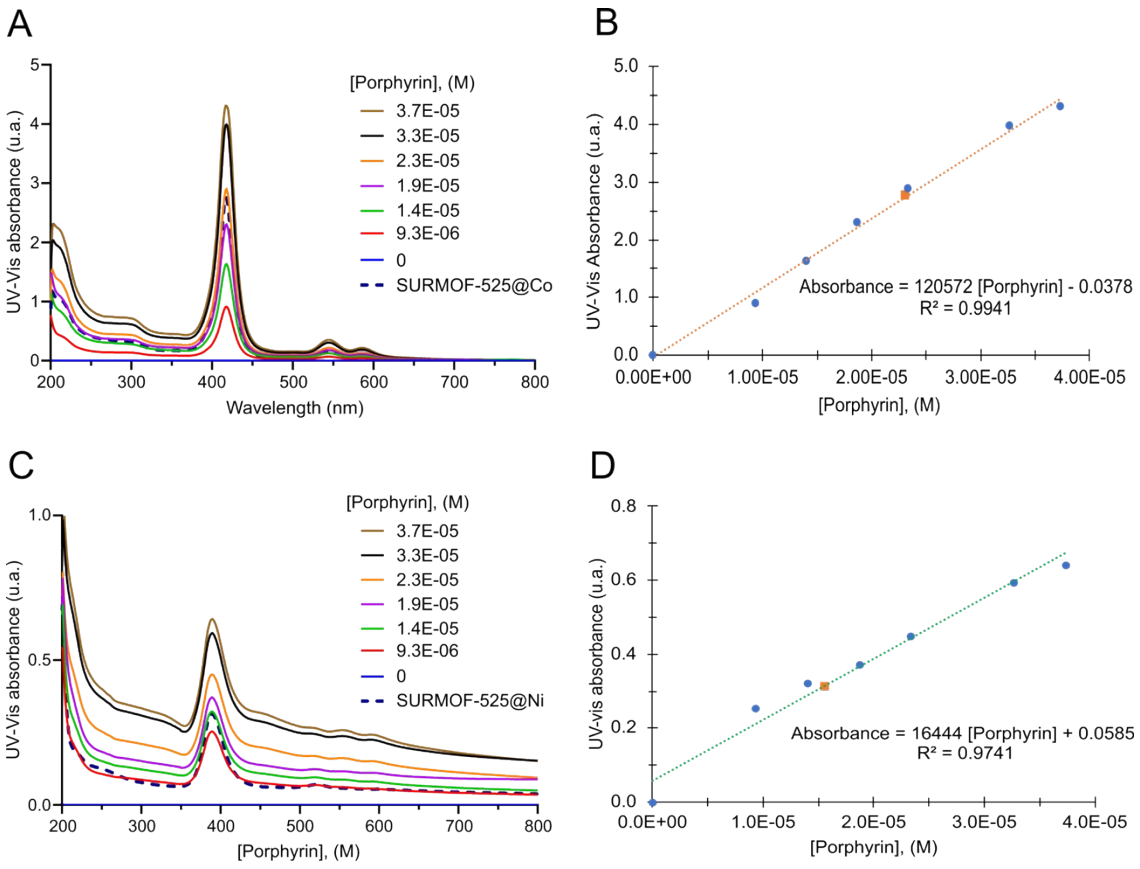

Fig. S6. A) UV-Vis absorption spectra of MOF525-@Co in NaOH 0.1M solution. B) The resulting calibration curve using the UV-Vis absorbance at 418 nm for the Porphyrin concentration in the MOF-525@Co. C) UV-Vis absorption spectra of MOF525-@Ni in NaOH 0.1M solution. D) The resulting calibration curve using the UV-Vis absorbance at 389 nm for

the Porphyrin concentration in the MOF-525@Ni. The spectra of SURMOF-525@Co in A) and SURMOF-525@Ni in C) were obtained letter digested each SURMOF in NaOH 0.1M

Estimation of molar extinction coefficient of the individual porphyrin for MOF-525@Co and MOF-525@Ni

The molar extinction coefficient was estimated by Lamber-Beer law at 418 nm for MOF-525@Co,

$$A^{\lambda = 418\ nm} = \varepsilon_{MOF-525@Co}^{\lambda = 418\ nm}\, l\, [Porphyrin]$$

Where *l* is the optical step length, (1 cm), according with Fig S6 B)

$$\varepsilon_{MOF-525@Co}^{\lambda = 418\ nm} = 120572 \frac{L}{cm * mol}$$

$$A^{\lambda = 418\ nm} = 120572 \frac{L}{cm * mol} (1\ cm) *\ [Porphyrin] - 0.0378$$

The absorbance by dilution of 50 µL of SURMOF-525@Co digested in 4 mL of NaOH 0.1 M at 418 nm is 2.7559

$$[Porphyrin]_{SURMOF-525@Co} = \frac{A^{\lambda = 418\ nm} + 0.0374}{(120572)} = \frac{2.7559 + 0.0374}{(120572)} = 2.35E-5\ M$$

$$V_i C_i = V_f C_f$$

$$[Porphyrin]_{diggested\ SURMOF-525@Co} = \frac{2\ mL * 2.35E-5\ M}{0.050\ mL} = 9.27\ E-4\ M$$

Or

$$[Porphyrin]_{diggested\ SURMOF-525@Co} = 0.93\ E-7\ \frac{mol}{cm^3}$$

$$\eta_{porphyrin\ in\ SURMOF-525@Co} = (0.93e-7) \frac{mol}{cm^3} * 4\ cm^3 = 3.71E-6\ mol$$

The area of SURMOF-525@Co electrode is 2 cm^2, thus porphyrin concentration in the working electrode is

$$[Porphyrin]_{WE,SURMOF-525@Co} = 1.85\ E-6\ \frac{mol}{cm^2}$$

considering that for every mol of SURMOF-525@Co there are 3 moles of porphyrin,

$$(SURMOF-525@Co) = 6.18\ E-7\ \frac{mol}{cm^2}$$

For SURMOF-525@Ni The molar extinction coefficient was estimated by Lamber-Beer law at 389 nm

$$A^{\lambda = 389\ nm} = \varepsilon^{\lambda = 389\ nm}_{MOF-525@Ni}\ l\ [Porphyrin]$$

According with Fig S6 D)

$$\varepsilon^{\lambda = 389\ nm}_{MOF-525@Ni} = \ 16444\frac{L}{cm * mol}$$

$$A^{\lambda = 389\ nm} = 16444\frac{L}{cm * mol}(1\ cm) *\ [Porphyrin]\frac{mol}{L} + 0.0585$$

The absorbance by dilution of 25 µL of SURMOF-525@Ni digested in 4 mL of NaOH 0.1 M at 389 nm is 0.3147

$$[Porphyrin]_{SURMOF-525@Ni} = \frac{A^{\lambda = 389\ nm} - 0.0585}{(16444)} = \frac{0.3147 - 0.0585}{(16444)} = 1.56E-5\ M$$

$$V_i C_i = V_f C_f$$

$$[Porphyrin]_{diggested\ SURMOF-525@Ni} = \frac{2\ mL * 1.56E-5\ M}{0.025\ mL} = 1.25\ E-3\ M$$

Or

$$[Porphyrin]_{diggested\ SURMOF-525@Ni} = 1.25\ E-6\ \frac{mol}{cm^3}$$

$$\eta_{porphyrin\ in\ SURMOF-525@Ni} = (1.25E-6)\frac{mol}{cm^3} * 4\ cm^3 = 5.0E-6\ mol$$

The area of SURMOF-525@Co electrode is 2 cm^2, thus porphyrin concentration in the working electrode is

$$[Porphyrin]_{WE,\ SURMOF-525@Ni} = 2.5\ E-6\ \frac{mol}{cm^2}$$

considering that for every mol of SURMOF-525@Ni there are 3 moles of porphyrin,

$$(SURMOF-525@Ni) = 8.3\ E-7\ \frac{mol}{cm^2}$$

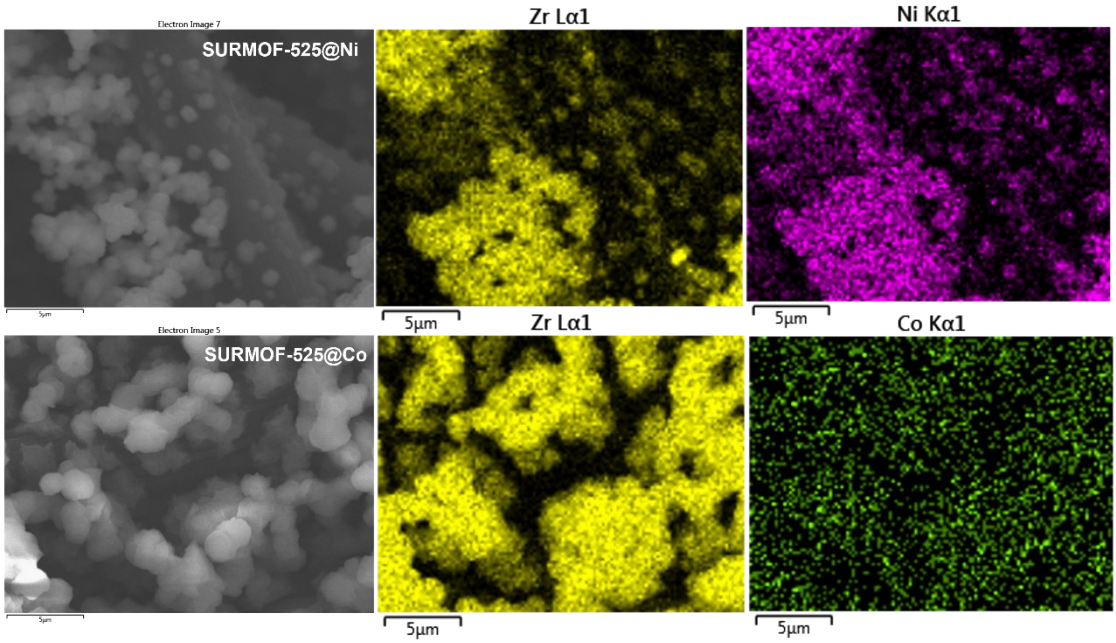

Fig. S7. EDS maps for SURMOF-525@Ni and SURMOF-525@Co.

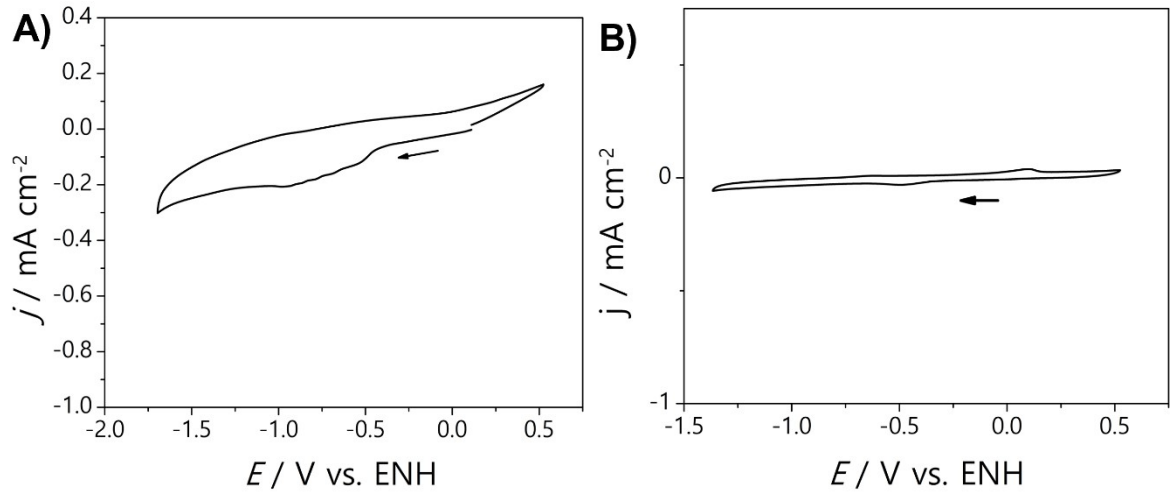

Fig. S8. Cyclic voltammograms of CP previously immersed in the metalation solution without the MOF. A) CP in cobalt metalation solution, B) CP in nickel metalation solution. The experiments were conducted in 0.3 M n-Bu_4NPF_6/MeCN solution and N_2 atmosphere (electrode geometric area = 2 cm^2).

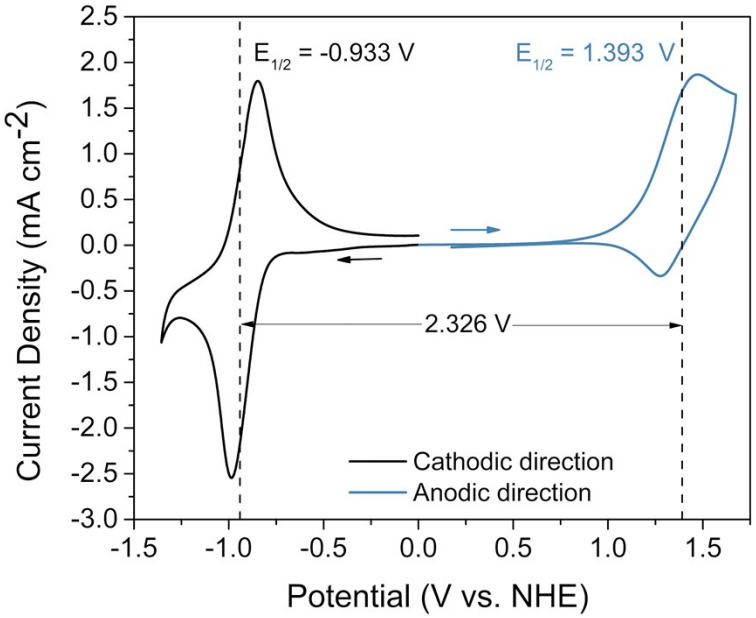

Fig. S9. Cyclic voltammograms of SURMOF-525@Ni in cathodic and anodic direction, *v* = 10 mV s^{-1}. The $\Delta E_{1/2}$ (Ox-Red) of 2.326 V it is used as a descriptor to locate the reduction and oxidation on macrocycle.[9] The experiments were conducted in 0.3 M n-Bu_4NPF_6/MeCN solution and N_2 atmosphere (electrode geometric area = 2 cm^2).

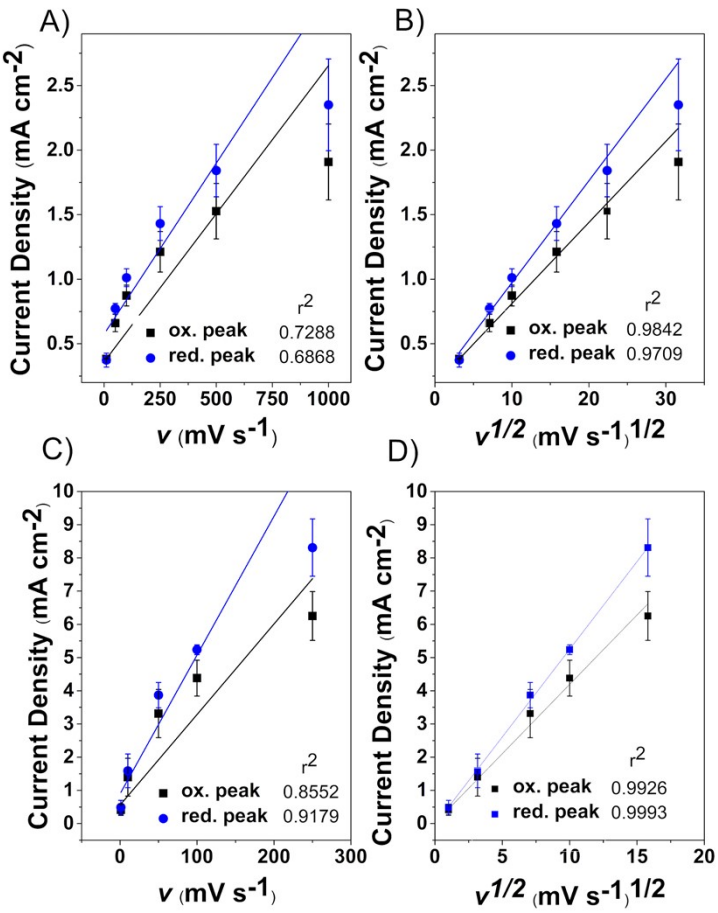

Fig. S10. (A) *v* vs current density graph for SURMOF-525@Co. (B) $v^{1/2}$ vs current density graph for SURMOF-525@Co. (C) *v* vs current density graph for SURMOF-525@Ni. (D) $v^{1/2}$ vs current density graph for SURMOF-525@Ni. The experiments were conducted in 0.3 M *n*-Bu_4NPF_6/MeCN solution and N_2 atmosphere (electrode geometric area = 2 cm^2).

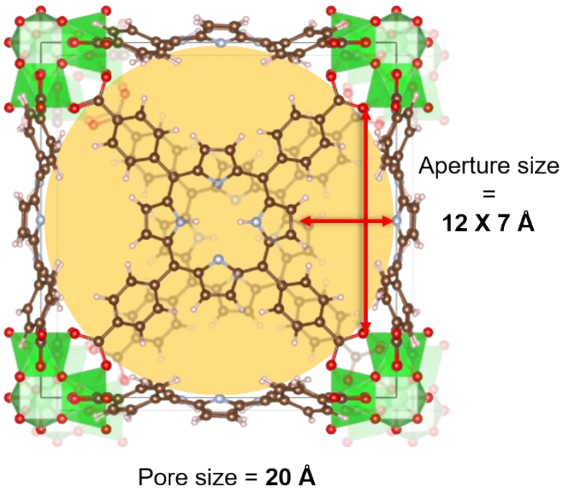

Fig. S11. Scheme of the crystal structure of MOF-525 showing the pore size and aperture size (formed between linker-linker and node-node).

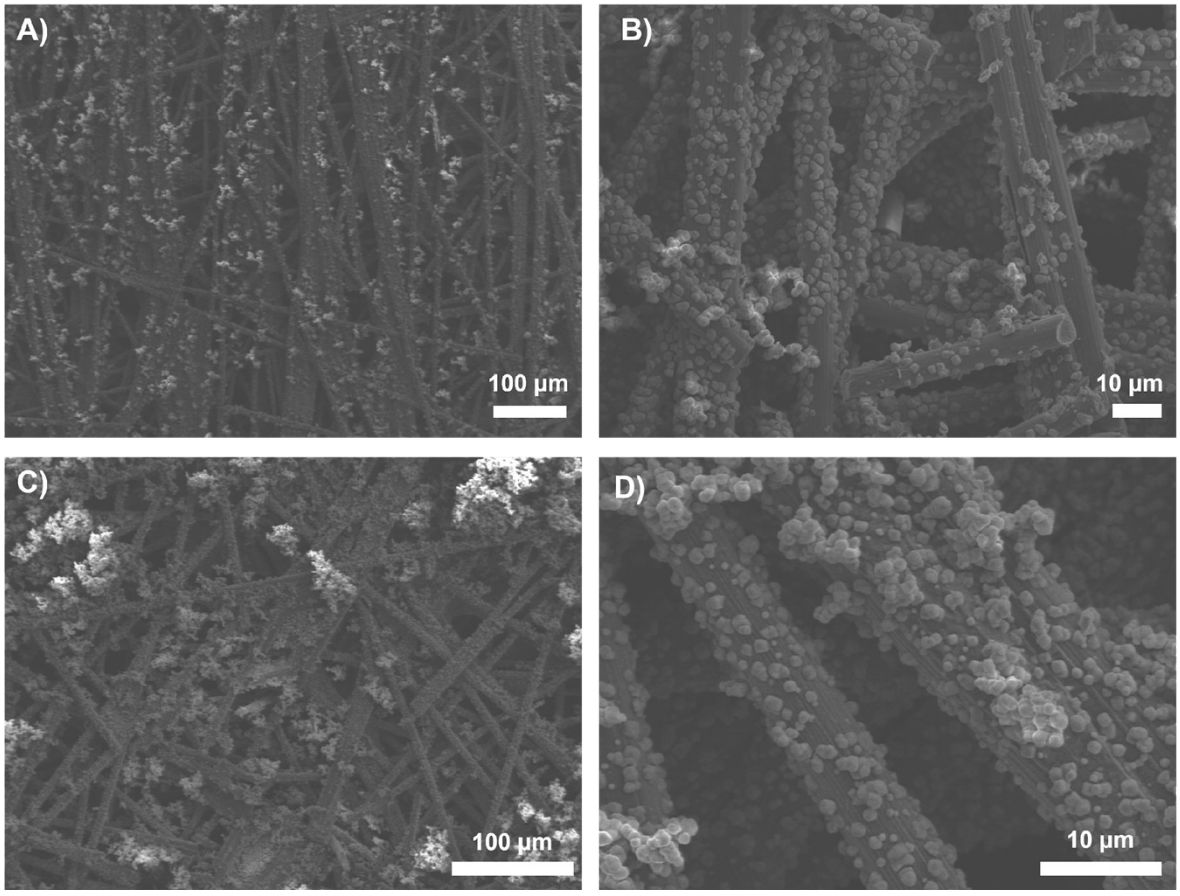

Fig. S12. SEM micrographs of MOF microcrystals distribution along cross-linked CP fibers (A, B) SURMOF-525@Co, (C, D) SURMOF-525@Ni.

Estimation of λ_o for MOF-525@M

The energy change associated with outer reorganization energy (λ_o) can be estimated through the equation[10–12]:

$$\lambda_0 = \frac{(\Delta e)^2}{8\pi\varepsilon_0}\left(\frac{1}{2r_D} + \frac{1}{2r_A} - \frac{1}{r_{AD}}\right)\left(\frac{1}{D_{op}} - \frac{1}{D_s}\right)$$

Where Δe is the charge transferred from donor to acceptor (e = electron charge = 1.6x10^{-19} C), $\boldsymbol{r_D}$ and $\boldsymbol{r_A}$ (m) are the radii of the π-electron cloud associated with the donor/acceptor (for MOF-525, $\boldsymbol{2r_{A/D}}$ is the size of the porphyrin core), $\boldsymbol{r_{AD}}$ (m) is the distance between the donor and acceptor (for MOF-525, the Metal-Metal or core-core distance). $\boldsymbol{D_{op}}$ is the square of the refractive index of the solvent, $\boldsymbol{D_s}$ it's the static dielectric constant of the solvent, and ε_0 (8.85x10^{-12} F/m) is the permittivity of the space.

For MOF-525 the size of the porphyrin core is 0.86 nm[10]. In the case of the metal-centred electrons transfer process (MOF-525@Co), the Co-Co distance is 1.37 nm. On the other hand, for the ring-centred electron transfer process (MOF-525@Ni), the core-core distance (from pyrrole-C_β to pyrrole-C_β) is 0.7 nm. The acetonitrile used as solvent/electrolyte has a $\boldsymbol{D_{op}}$ of 1.8 and a $\boldsymbol{D_s}$ of 37.5.

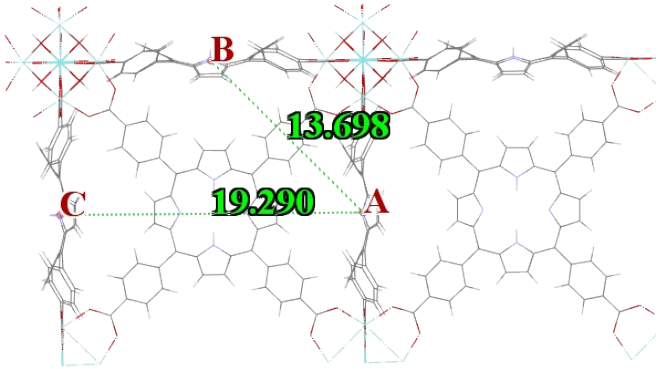

Estimation of distances (Å) between adjacent linkers (Metal to Metal) in MOF-525 using Mercury.

For MOF-525@Co:

$$\lambda_0 = \frac{(1.6x10^{-19}C)^2}{8\pi(8.85x10^{-12}\frac{F}{m})}\left(\frac{1}{0.86x10^{-9}m} + \frac{1}{0.86x10^{-9}m} - \frac{1}{1.37x10^{-9}m}\right)\left(\frac{1}{1.8} - \frac{1}{37.5}\right) = 0.607\ eV$$

For MOF-525@Ni:

$$\lambda_0 = \frac{(1.6x10^{-19}C)^2}{8\pi(8.85x10^{-12}\frac{F}{m})}\left(\frac{1}{0.86x10^{-9}m} + \frac{1}{0.86x10^{-9}m} - \frac{1}{0.7x10^{-9}m}\right)\left(\frac{1}{1.8} - \frac{1}{37.5}\right) = 0.341\ eV$$

3. References

1 I. Hod, M. D. Sampson, P. Deria, C. P. Kubiak, O. K. Farha and J. T. Hupp, *ACS Catal.*, 2015, **5**, 6302–6309.

2 W. Morris, B. Volosskiy, S. Demir, F. Gándara, P. L. McGrier, H. Furukawa, D. Cascio, J. F. Stoddart and O. M. Yaghi, *Inorg. Chem.*, 2012, **51**, 6443–6445.

3 S. Balakrishnan, A. J. Downard and S. G. Telfer, *J. Mater. Chem.*, 2011, **21**, 19207–19209.

4 C. Hou, J. Peng, Q. Xu, Z. Ji and X. Hu, *RSC Adv.*, 2012, **2**, 12696–12698.

5 C. Saby, B. Ortiz, G. Y. Champagne and D. Bélanger, *Langmuir*, 2002, **13**, 6805–6813.

6 D. W. Thomas and A. E. Martell, *J. Am. Chem. Soc.*, 1959, **81**, 5111–5119.

7 S. Carrasco, A. Sanz-Marco and B. Martín-Matute, *Organometallics*, 2019, **38**, 3429–3435.

8 D. F. Marsh and L. M. Mink, *J. Chem. Educ.*, 1996, **73**, 1188–1190.

9 D. Chang, T. Malinski, A. Ulman and K. M. Kadish, *Inorg. Chem.*, 1984, **23**, 817–824.

10 S. Patwardhan and G. C. Schatz, *J. Phys. Chem. C*, 2015, **119**, 24238–24247.

11 K. B. Ørnsø, E. O. Jónsson, K. W. Jacobsen and K. S. Thygesen, *J. Phys. Chem. C*, 2015, **119**, 12792–12800.

12 V. May and O. Kuhn, *Charge and Energy Transfer Dynamics in Molecular Systems*, Wiley-VCH Verlag GmbH & Co. KGaA, Third., 2011.